Electronic Supplementary Information for:

Cationic gemini lipids containing polyoxyethylene spacers as improved transfecting agents of plasmid DNA in cancer cells

Ana L. Barrán-Berdón,[†,‡] Santosh K. Misra,[§,‡] Sougata Datta,[§,†] Mónica Muñoz-Úbeda,[†] Paturu Kondaiah, [#] Elena Junquera,[†] Santanu Bhattacharya,*[,§] and Emilio Aicart*[,†]

[†]Grupo de Química Coloidal y Supramolecular, Departamento de Química Física I, Facultad de Ciencias Químicas, Universidad Complutense de Madrid, 28040 Madrid, Spain

Departments of [§]Organic Chemistry, and [#]Molecular Reproduction Development and Genetics, Indian Institute of Science, 560012 Bangalore, India

[‡]These authors contributed equally

*Authors to whom the correspondence should be addressed:
Santanu Bhattacharya: Fax: +918023600529. e-mail: sb@orgchem.iisc.ernet.in
Emilio Aicart: Fax: +34913944135. e-mail: aicart@quim.ucm.es

Synthesis of the Bis(hexadecyl dimethyl ammonium) oxyethylene surfactants

Scheme 1 The synthetic route to 1a-c [a]

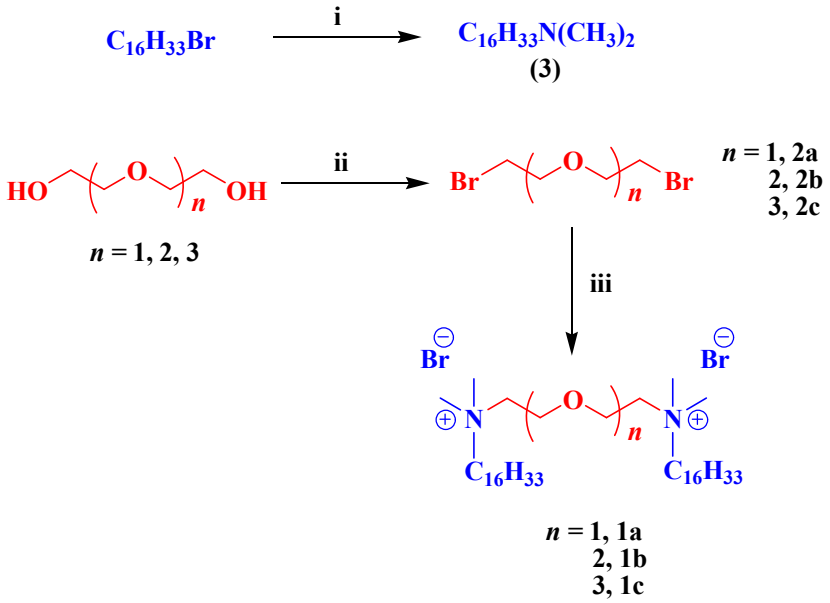

[a] (i) NMe_2, ethanol, reflux, 80 ºC, 24 h, yield ~90%; (ii) PBr_3, 50-60 ºC, 12 h, yield ~80% (n = 1), 85% (n = 2), 90% (n = 3); (iii) $C_{16}NMe_2$, dry ethanol, sealed tube, 80 ºC, 72 h, ~80% (n = 1), 75% (n = 2), 70% (n = 3).

All the reagents and solvents used for the present study were of highest grade available commercially and used purified, dried or freshly distilled as required. *n*-Hexadecyl bromide, PBr_3 and diols were bought from Aldrich chemical company. Each synthesized compound was characterized by ^{1}H-NMR spectra recorded in $CDCl_3$ in Bruker 400 MHz NMR spectrometer. Chemical shifts (δ) are reported in ppm downfield from the internal standard (TMS). Elemental analysis was recorded in Thermo Finnigan EA FLASH 1112 SERIES.

N-*n*-Hexadecyl-*N*,*N*-dimethylamine (3). *n*-Hexadecyl bromide (10 g, 32.74 mmol) and dimethylamine (40% aq solution, 22 mL, 98.24 mmol) were refluxed in ethanol at ~80 ^{o}C for 24 h. Then the reaction mixture was extracted with $CHCl_3$ (50 mL × 3) and the combined organic layer was washed with water (50 mL) and brine (50 mL). The organic layer was separated and dried over anhydrous Na_2SO_4. Solvent was evaporated to leave a residue. A pure product was obtained after column chromatography using silica gel (60-120 mesh) with 5-10% EtOAc/hexane as eluent. 7.94 g (29.46 mmol), yield = 90%. ^{1}H-NMR ($CDCl_3$, 400 MHz, TMS, rt): δ 0.88 (t, 3H), 1.25-1.28 (br s, 26H), 1.43-1.46 (t, 2H), 2.21-2.25 (m, 8H).

Synthesis of dibromides (2a-c). The dibromides (**2a-c**) were synthesized as described in the following. All the dibromides were obtained by the drop wise addition of PBr_3 (37.69 mmol) to the each diol (47.11 mmol) over a period of 1 h at 0 °C. Then, the reaction mixtures were allowed to come to room temperature and subsequently heated at 50-60 °C for 12 h. After that, the reaction mixture was cooled and diluted with $CHCl_3$. The resultant organic layer was washed with water, $NaHCO_3$ and again with water and finally dried over anhydrous Na_2SO_4. Solvent was evaporated and the crude product was purified on a silica gel column (60-120 mesh) using hexane as eluent to get a colourless liquid. The overall yields of the dibromides ranged from 80-90%.

Bis(2-bromo ethyl) ether (**2a).** ^{1}H-NMR ($CDCl_3$, 400 MHz, TMS, rt): δ 3.48 (t, 4H), 3.84 (t, 4H).

1,2-Bis(2-bromo ethoxy) ethane (2b). ^{1}H-NMR ($CDCl_3$, 400 MHz, TMS, rt): δ 3.48 (t, 4H), 3.69 (s, 4H), 3.88 (t, 4H).

Bis(5-bromo ethoxy ethyl) ether (2c). ^{1}H-NMR ($CDCl_3$, 400 MHz, TMS, rt): δ 3.45 (t, 4H), 3.65 (s, 8H), 3.81 (t, 4H).

Synthesis of Bis(quaternary ammonium) surfactants (1a-c). The bis(quaternary ammonium) surfactants were synthesized as described in the previous reports.[1] All the surfactants **1a-c** were obtained by refluxing the corresponding α,ω-dibromoalkoxyalkanes (1.315 mmol) with *N*-*n*-hexadecyl-*N*,*N*-dimethylamine (3.95 mmol) in dry ethanol at 80 ºC in a sealed tube for 72 h. After that, the ethanol was completely removed under vacuum from the reaction mixture and the solid residue obtained was dissolved in minimum volume of chloroform and precipitated several times by drop wise addition in ethyl acetate. The overall yields of the surfactants ranged from 70-80%.

Bis(hexadecyl dimethyl ammonium) diethyl ether (1a). ^{1}H-NMR ($CDCl_3$, 400 MHz, TMS, rt) : δ 0.88 (t, 6H), 1.25-1.35 (s + br m, 52H), 1.72 (br s, 4H), 3.44 (s, 12H), 3.62 (t, 4H), 4.01 (br s, 4H), 4.33 (br s, 4H); Elemental analysis calcd. for $C_{40}H_{86}N_2OBr_2$, 0.5 H_2O: C 61.62, H 10.99, N 3.59. Found: C 61.33, H 11.24, N 3.48.

Bis(hexadecyl dimethyl ammonium) diethoxy ethane (1b). ^{1}H-NMR ($CDCl_3$, 400 MHz, TMS, rt) : δ 0.88 (t, 6H), 1.25-1.35 (s + br m, 52H), 1.74 (br s, 4H), 3.44 (s, 12H), 3.50-3.63 (m, 4H), 3.97 (br s, 4H), 4.16 (br s, 4H), 4.33 (br s, 4H); Elemental analysis calcd. for $C_{42}H_{90}N_2O_2Br_2$, H_2O: C 60.56, H 11.13, N 3.36. Found: C 60.51, H 11.27, N 3.03.

Bis(hexadecyl dimethyl ammonium)bis(ethoxy ethyl) ether (1c).[1,2] ^{1}H-NMR ($CDCl_3$, 400 MHz, TMS, rt) : δ 0.88 (t, 6H), 1.25-1.35 (s + br m, 52H), 1.72 (br s, 4H), 3.45 (s, 12H), 3.61-3.65 (t, 8H), 4.02 (br s, 8H), 4.35 (br s, 4H); Elemental analysis calcd. for $C_{44}H_{94}N_2O_3Br_2$: C 61.52, H 11.03, N 3.26. Found: C 61.62, H 11.33, N 3.13.

Preparation of lipid mixtures and lipoplexes. Appropriate amounts of gemini surfactant (L^+) and DOPE (L^0) were dissolved in chloroform to obtain the desired GCL composition (α) of the mixed liposomes. The resulting dry lipid films were then hydrated with HEPES, pH = 7.4, and homogenized with the help of alternating cycles of vigorous vortexing, sonication and moderate heat to transformed into the desired unilamellar liposomes (LUVs) by a sequential extrusion procedure, widely explained elsewhere.[3] A stock solution of pDNA concentration were determined by absorbance at 260 nm (ε = 6600 $M^{-1}cm^{-1}$).[4]

In order to obtain the desired lipoplex composition (in terms of total lipid to pDNA mass ratio (L/D) or the effective charge ratio (ρ_{eff}) between the GCL and pDNA), equal volumes of pDNA and $(C_{16}Am)_2(C_2O)_n$ (n = 1, 2 or 3) extruded liposomal suspensions were mixed by adding pDNA over mixed liposomes. The mixing process was done at an addition speed of 0.2 mL/min, with continuous, constant, and vigorous magnetic stirring. Once the addition was concluded, the solution was maintained under agitation during 10 min to favor the formation of lipoplexes.

Gel electrophoresis. Lipoplexes along with uncomplexed, plasmid DNA were loaded on to 1% agarose gel and run for 20 min at 120 mV in 1x TAE (Tris-HCl, Acetate and EDTA) buffer. Same amount of pDNA (200 ng; free and complexed) was used per well for all the samples. Then, gels were photographed under UV light illumination at 365 nm for 3.5 sec. Fully complexed lipoplexes retained in the wells of the gel, while uncomplexed pDNA appeared as a bright band outside of the well. Fluorescence intensity of each band was measured by using commercial Alfa-digi-Doc software provided with Gel-Doc instrument (UV-pro-Platinum). The band intensity for the free pDNA was considered as 100% and other intensities were estimated accordingly.

Transfection of pDNA. Transfection of pEGFP-C3 plasmid DNA across HEK293T (Human embryo kidney transformed cancer), HeLa (Human cervical cell carcinoma), CaCO-2 (Human epithelial colorectal adenocarcinoma), Hep3B (Human hepatoma) and MAD-MB231 (Human breast cancer) cells using lipid mixtures $(C_{16}Am)_2(C_2O)_n$ (n = 1, 2 or 3) was performed in absence (-FBS-FBS) and presence (-FBS+FBS) of serum. Lipoplexes were prepared using 0.1 μg/μL of pDNA diluted with plain DMEM (Sigma-Aldrich). The amount of mixed lipids was added to 0.8 μg of pDNA in such a way that the desired effective charge ratio (ρ_{eff}) was obtained. The volume of the mixture was made up to 100 μL with plain DMEM. After 30 min of incubation at room temperature, the lipoplex suspension was further diluted with either 100 μL of plain DMEM without serum (-FBS-FBS) or with 100 μL of 20% FBS containing DMEM (-FBS+FBS). Then 200 μL of lipoplex suspensions with or without FBS added to each well of 24 wells plated with ~60,000 cells. Experiments were performed in duplicate and repeated twice independently for each ρ_{eff}. After 6 h of incubation at ambient condition, old medium was replaced with 500 μL 10% FBS containing DMEM. Cells were further incubated for ~48 h. GFP expressions were followed by fluorescence microscopic studies under fluorescent microscopy. Cells were harvested by trypsinization in 2% FBS containing DPBS. Collected cells were carried for Flow Assisted Cell Sorting (FACS) to obtain % GFP positive cells as well as the average intensity of fluorescence per cell (Mean Fluorescence Intensity (MFI). Data were analyzed using public domain software WinMDI 2.8. Results were plotted as % GFP cells and MFI against effective charge ratio (ρ_{eff}) on Graph pad prism 5.0 software. Lipofectamine2000 was used as a positive control during all the transfection experiments.

Transfection efficiency by fluorescence microscopy. To observe the GFP gene expression efficiency, fluorescence microscopy was performed on IX81, Olympus fluorescence microscope. Cells were observed and photographed after 48 h of incubation. Cells were transfected as mentioned above using optimized lipoplexes in absence (–FBS-FBS) and presence of serum (-FBS+FBS) conditions while Lipo2000* was used as positive control.

Confocal fluorescence microscopy (CFM). CFM Study was performed on HEK293T cells by transfecting pEGFP-C3 plasmid and nuclear staining with PI. It tells the qualitative differences in GFP expression and in turn gene transfection efficiency of various formulations. The experiments were performed in similar way as described earlier. Control experiments were performed in each case using commercial transfection reagent, Lipo2000* Samples were observed under confocal microscope (Zeiss LSM 510-Meta Apochromat).

Cell viability assay. The cytotoxicity or cell viability of each lipid formulation toward HEK293T cells was determined by using 3-(4,5-dimethylthiazole-2-yl)-2,5-diphenyl tetrazolium bromide reduction method (MTT assay) following literature procedure.[5] The absorbance was measured using a microtiter plate reader. The % cell viability was then calculated from readings obtained from ELISA reader using formula

$$\% \text{ Viability} = \frac{A_{590,\text{treated cells}} - A_{590,\text{background}}}{A_{590,\text{untreated cells}} - A_{590,\text{background}}} \text{ x } 100 \qquad (1)$$

Determination of the effective charges of the CL and plasmid DNA, and the electroneutrality of the lipoplex

Liposome composition is given as the CL molar fraction (α) while either the total lipid to DNA mass ratio (L/D) or the effective charge ratio (ρ_{eff}) between the charges of positive CL and negative DNA phosphate groups are used to define the composition of the lipoplex. These quantities are related by the following equations:

$$\alpha = \frac{L^+ / M_{L^+}}{(L^+ / M_{L^+}) + (L^0 / M_{L^0})} \quad (2)$$

$$\rho_{eff} = \frac{n^+}{n^-} = \frac{q^+_{L^+} L^+ / M_{L^+}}{q^-_{DNA} D / \overline{M}_{bp}} \quad (3)$$

where M_{L^+} and M_{L^0} are the molar masses of cationic and helper lipids; n^+ and n^- are the number of moles of positive and negative charges, of CL and DNA; $q^+_{L^+}$ and q^-_{DNA} are the charges of CL and DNA per bp; and $\overline{M}_{bp}$ is the average molar mass of DNA bp. Because efficient cell transfection requires net positive lipoplex to cross the negative cell membrane, there is one L/D value, called electroneutrality ratio ($(L/D)_\phi$) where both charges balance (ρ_{eff} = 1); this ratio marks the lower limit from which the lipoplex becomes a potentially efficient cell transfecting agent.[6,7] Zeta potential (ζ), related with the net charge of the lipoplex, is the best physicochemical property to provide this information. Fig. 1a and Fig. S1 of the ESI show plots of ζ vs. L/D at several α values for the three GCLs used in this work. The electroneutrality ratio $(L/D)_\phi$ of the lipoplex can be determined as the L/D where a sign inversion on the charge occurs on the ζ sigmoidal profiles. This value is related with the previous quantities by:

$$\left(\frac{L}{D}\right)_{\phi} = \frac{q^{-}_{DNA}\left[\alpha M_{L^+} + (1-\alpha)M_{L^0}\right]}{q^{+}_{L^+}\alpha\overline{M}_{bp}} \qquad (4)$$

Studies reported in literature have shown that commercial linear DNA, as calf thymus DNA, or so on, has its negative charge totally available for the CL, i.e., $q^{-}_{linearDNA}$ = -2 per bp. But experiments recently reported by us,[8-11] have demonstrated that, at physiological conditions, plasmid DNA remains in a supercoiled conformation[12,13] rendering a much less negative charge than its nominal one ($q^{-}_{pDNA} << -2$). For that reason, any biophysical or biological lipoplexes study must start with the determination of the effective charge of both, the CL ($q^{+}_{L^+}$) and the pDNA (q^{-}_{pDNA}).

Initially, the effective charge of the CL ($q^{+}_{L^+}$) can be determined for a certain GCL composition (α) of the mixed liposome, from eq 4 using the $(L/D)_{\phi}$ value of the GCL/DOPE-linear DNA lipoplex experimentally measured from zeta potential, and assuming $q^{-}_{linearDNA}$ = -2. Once $q^{+}_{L^+}$ is known, the measurement of $(L/D)_{\phi}$ for the GCL/DOPE-pDNA lipoplex, but now containing plasmid DNA in identical mixed lipid composition (α) (Fig. 1, Fig. S1 and Table S1 of ESI) must be carried on, because it permits the determination of the effective charge of the plasmid DNA (q^{-}_{pDNA}) using eq 5 after rearranging eq 4:

$$q^{-}_{pDNA} = \left(\frac{L}{D}\right)_{\phi}\left(\frac{q^{+}_{L^+}\alpha\overline{M}_{bp}}{\left[\alpha M_{L^+} + (1-\alpha)M_{L^0}\right]}\right) \qquad (5)$$

The effective charge of pDNA (q^{-}_{pDNA}) can been also obtained from gel electrophoresis experiments (Figure S2, as an example) although with higher uncertainty.

Once the real charges $q^{+}_{L^+}$ and q^{-}_{pDNA} are correctly obtained, the effective charge ratio (ρ_{eff}) of the lipoplex, between the GCL positive charges and the pDNA negative ones, may

be also calculated by substituting $q^{+}_{L^{+}}$ and q^{-}_{pDNA} in eq 3. The ρ_{eff} quantity is the key to prepare lipoplexes with optimum performances toward transfection, i.e., with a net positive charge and with the lowest level of cytotoxicity.

Notes and references

1 A. Pal, S. Datta, V. K. Aswal and S. Bhattacharya, *J. Phys. Chem. B*, 2012, **116**, 13239-13247.
2 S. De, V. K. Aswal, P. S. Goyal and S. Bhattacharya, *J. Phys. Chem. B*, 1998, **102**, 6152-6160.
3 A. Rodriguez-Pulido, F. Ortega, O. Llorca, E. Aicart and E. Junquera, *J. Phys. Chem. B*, 2008, **112**, 12555-12565.
4 M. B. Hansen, S. E. Nielsen and K. Berg, *J. Immunol. Methods*, 1989, **119**, 203-210.
5 A. Bajaj, P. Kondiah and S. Bhattacharya, *J. Med. Chem.*, 2007, **50**, 2432-2442.
6 R. S. Dias and B. Lindman, *DNA Interaction with Polymers and Surfactants*, Wiley & Sons, Hoboken, 2008.
7 A. Rodriguez-Pulido, A. Martin-Molina, C. Rodriguez-Beas, O. Llorca, E. Aicart and E. Junquera, *J. Phys. Chem. B*, 2009, **113**, 15648-15661.
8 M. Muñoz-Ubeda, S. K. Misra, A. L. Barran-Berdon, C. Aicart-Ramos, M. B. Sierra, J. Biswas, P. Kondaiah, E. Junquera, S. Bhattacharya and E. Aicart, *J. Am. Chem. Soc.*, 2011, **133**, 18014-18017.
9 A. L. Barran-Berdon, M. Muñoz-Ubeda, C. Aicart-Ramos, L. Perez, M. R. Infante, P. Castro-Hartmann, A. Martin-Molina, E. Aicart and E. Junquera, *Soft Matter*, 2012, **8**, 7368-7380.
10 M. Muñoz-Ubeda, S. K. Misra, A. L. Barran-Berdon, S. Data, C. Aicart-Ramos, P. Castro-Hartmann, P. Kondaiah, E. Junquera, S. Bhattacharya and E. Aicart, *Biomacromolecules*, 2012, **13**, 3926-3937.
11 S. K. Misra, M. Munoz-Ubeda, S. Datta, A. L. Barran-Berdon, C. Aicart-Ramos, P. Castro-Hartmann, P. Kondaiah, E. Junquera, S. Bhattacharya and E. Aicart, *Biomacromolecules*, 2013, **14**, 3951-3963.
12 Y. L. Lyubchenko and L. S. Shlyakhtenko, *Proc. Natl. Acad. Sci. U.S.A.*, 1997, **94**, 496-501.
13 M. Foldvari, I. Badea, S. Wettig, R. Verrall and M. Bagonluri, *J. Exp. Nanosci.*, 2006, **1**, 165-176.

Table S1 Values of the cationic lipid charge ($q^{+}_{L^{+}}$) and the effective pDNA charge (q^{-}_{pDNA}) for $(C_{16}Am)_2(C_2O)_n$/DOPE-pDNA, experimentally obtained from zeta potential for the three series (with n = 1, 2 or 3) studied in this work

n	α	$q^{+}_{L^{+}}$	q^{-}_{pDNA}
1	0.2	1.70	-0.4
	0.4	1.70	-0.5
	0.5	1.70	-0.6
	0.7	1.70	-0.8
2	0.2	1.75	-0.3
	0.4	1.75	-0.4
	0.5	1.75	-0.4
	0.7	1.75	-0.4
3	0.2	1.80	-0.3
	0.4	1.80	-0.3
	0.5	1.80	-0.3
	0.7	1.80	-0.2

Table S2 Values of the particle size and the polydispersity for the mixed liposomes $(C_{16}Am)_2(C_2O)_n$/DOPE, with n = 1, 2 or 3, at several GCL compositions (α) determined from PALS technique

n	α	Size/nm	Polydispersity
1	0.2	103	0.05
	0.5	90	0.13
	0.7	75	0.16
2	0.2	107	0.04
	0.5	89	0.09
	0.7	72	0.26
3	0.2	106	0.04
	0.5	91	0.10
	0.7	79	0.21

Table S3 Values of the bigger, medium and lower particle sizes, for the mixed liposomes $(C_{16}Am)_2(C_2O)$/DOPE, at several GCL compositions (α) determined from cryo-TEM

Group	Size / nm	Percentage / %	
		α = 0.2	α = 0.5
Bigger size	110± 10	55	36
Medium size	80 ± 8	39	43
Lower size	50 ± 5	6	21

Table S4 Values of q_{100}, d_{100}, q_{pDNA} and d_{pDNA} of the lamellar (L_α) structures found for $(C_{16}Am)_2(C_2O)$/DOPE-pDNA at several GCL compositions (α) of the mixed lipid and at several effective charge ratios (ρ_{eff})

$(C_{16}Am)_2(C_2O)$/DOPE-pDNA								
ρ_{eff}		α						
		0.2		0.4		0.5	0.7	
		$L_{\alpha\ DOPE\ rich}$	$L_{\alpha\ main}$	$L_{\alpha\ DOPE\ rich}$	$L_{\alpha\ main}$	$L_{\alpha\ main}$	$L_{\alpha\ main}$	$L_{\alpha\ GCL\ rich}$
1.5	q_{100}	0.76	0.94	0.75	1.01	1.03	1.05	1.15
	d_{100}	8.27	6.68	8.38	6.22	6.10	5.98	5.46
	q_{pDNA}		1.28		1.35	1.46	1.66	
	d_{pDNA}		4.91		4.65	4.30	3.79	
2.0	q_{100}	0.75	0.94	0.75	1.01	1.04	1.05	1.16
	d_{100}	8.38	6.68	8.38	6.22	6.04	5.98	5.42
	q_{pDNA}		1.28		1.35	1.46	1.66	
	d_{pDNA}		4.91		4.65	4.30	3.79	
2.5	q_{100}	0.76	0.94	0.75	1.01	1.04	1.05	1.15
	d_{100}	8.27	6.68	8.38	6.22	6.04	5.98	5.46
	q_{pDNA}		1.27		1.34	1.46	1.66	
	d_{pDNA}		4.95		4.69	4.30	3.79	
3.0	q_{100}	0.75	0.94	0.75	1.01	1.04	1.05	1.15
	d_{100}	8.38	6.68	8.38	6.22	6.04	5.98	5.46
	q_{pDNA}		1.28		1.35	1.46	1.66	
	d_{pDNA}		4.91		4.65	4.30	3.79	
5.0	q_{100}	0.73	0.94	0.73	1.01	1.04	1.06	1.16
	d_{100}	8.61	6.68	8.61	6.22	6.04	5.93	5.42
	q_{pDNA}		1.28		1.34	1.46	1.66	
	d_{pDNA}		4.91		4.69	4.30	3.79	

Table S5 Values of q_{100}, d_{100}, q_{pDNA} and d_{pDNA} of the lamellar (L_α) structures found for $(C_{16}Am)_2(C_2O)_2$/DOPE-pDNA at several GCL compositions (α) of the mixed lipid and at several effective charge ratios (ρ_{eff})

$(C_{16}$Ammonium$)_2(C_2O)_2$/DOPE-pDNA							
ρ_{eff}		α					
		0.2		0.4	0.5	0.7	
		L_{α} DOPE rich	L_{α} main	L_{α} main	L_{α} main	L_{α} main	L_{α} GCL rich
1.5	q_{100}	0.74	0.93	1.01	1.05	1.11	1.16
	d_{100}	8.49	6.76	6.22	5.98	5.66	5.42
	q_{pDNA}		1.32	1.40	1.54	1.68	
	d_{pDNA}		4.76	4.49	4.08	3.74	
2.0	q_{100}	0.73	0.94	1.02	1.05	1.11	1.16
	d_{100}	8.61	6.68	6.16	5.98	5.66	5.42
	q_{pDNA}		1.33	1.40	1.55	1.68	
	d_{pDNA}		4.72	4.49	4.05	3.74	
2.5	q_{100}	0.74	0.94	1.01	1.05	1.09	1.16
	d_{100}	8.49	6.68	6.22	5.98	5.76	5.42
	q_{pDNA}		1.33	1.39	1.55	1.68	
	d_{pDNA}		4.72	4.52	4.05	3.74	
3.0	q_{100}	0.72	0.94	1	1.06	1.11	1.16
	d_{100}	8.73	6.68	6.28	5.93	5.66	5.42
	q_{pDNA}		1.33	1.40	1.55	1.68	
	d_{pDNA}		4.72	4.49	4.05	3.74	
5.0	q_{100}	0.72	0.94	1.01	1.06	1.1	1.16
	d_{100}	8.73	6.68	6.22	5.93	5.71	5.42
	q_{pDNA}		1.33	1.49	1.55	1.68	
	d_{pDNA}		4.72	4.22	4.05	3.74	

Table S6 Values of q_{100}, d_{100}, q_{pDNA} and d_{pDNA} of the lamellar (L_α) structures found for $(C_{16}Am)_2(C_2O)_3$/DOPE-pDNA at several GCL compositions (α) of the mixed lipid and at several effective charge ratios (ρ_{eff})

$(C_{16}Am)_2(C_2O)_3$/DOPE-pDNA							
ρ_{eff}		α					
		0.2		0.4	0.5	0.7	
		$L_{\alpha\ DOPE\ rich}$	$L_{\alpha\ main}$	$L_{\alpha\ main}$	$L_{\alpha\ main}$	$L_{\alpha\ main}$	$L_{\alpha\ GCL\ rich}$
1.5	q_{100}	0.86	0.94	1.01	1.04	1.06	1.16
	d_{100}	7.31	6.71	6.25	6.06	5.94	5.42
	q_{pDNA}		1.29	1.34	1.42	1.68	
	d_{pDNA}		4.87	4.69	4.42	3.74	
2.0	q_{100}	0.85	0.94	1.01	1.03	1.05	1.16
	d_{100}	7.37	6.71	6.24	6.08	5.97	5.42
	q_{pDNA}		1.29	1.35	1.42	1.68	
	d_{pDNA}		4.87	4.65	4.42	3.74	
2.5	q_{100}	0.87	0.93	1.01	1.04	1.05	1.16
	d_{100}	7.25	6.74	6.23	6.03	6.00	5.42
	q_{pDNA}		1.29	1.35	1.42	1.68	
	d_{pDNA}		4.87	4.65	4.42	3.74	
3.0	q_{100}	0.87	0.93	1.01	1.04	1.05	1.16
	d_{100}	7.24	6.74	6.22	6.03	6.00	5.42
	q_{pDNA}		1.29	1.34	1.42	1.68	
	d_{pDNA}		4.87	4.69	4.42	3.74	
5.0	q_{100}	0.86	0.94	1.01	1.04	1.05	1.16
	d_{100}	7.31	6.71	6.21	6.03	6.00	5.42
	q_{pDNA}		1.29	1.34	1.42	1.68	
	d_{pDNA}		4.87	4.69	4.42	3.74	

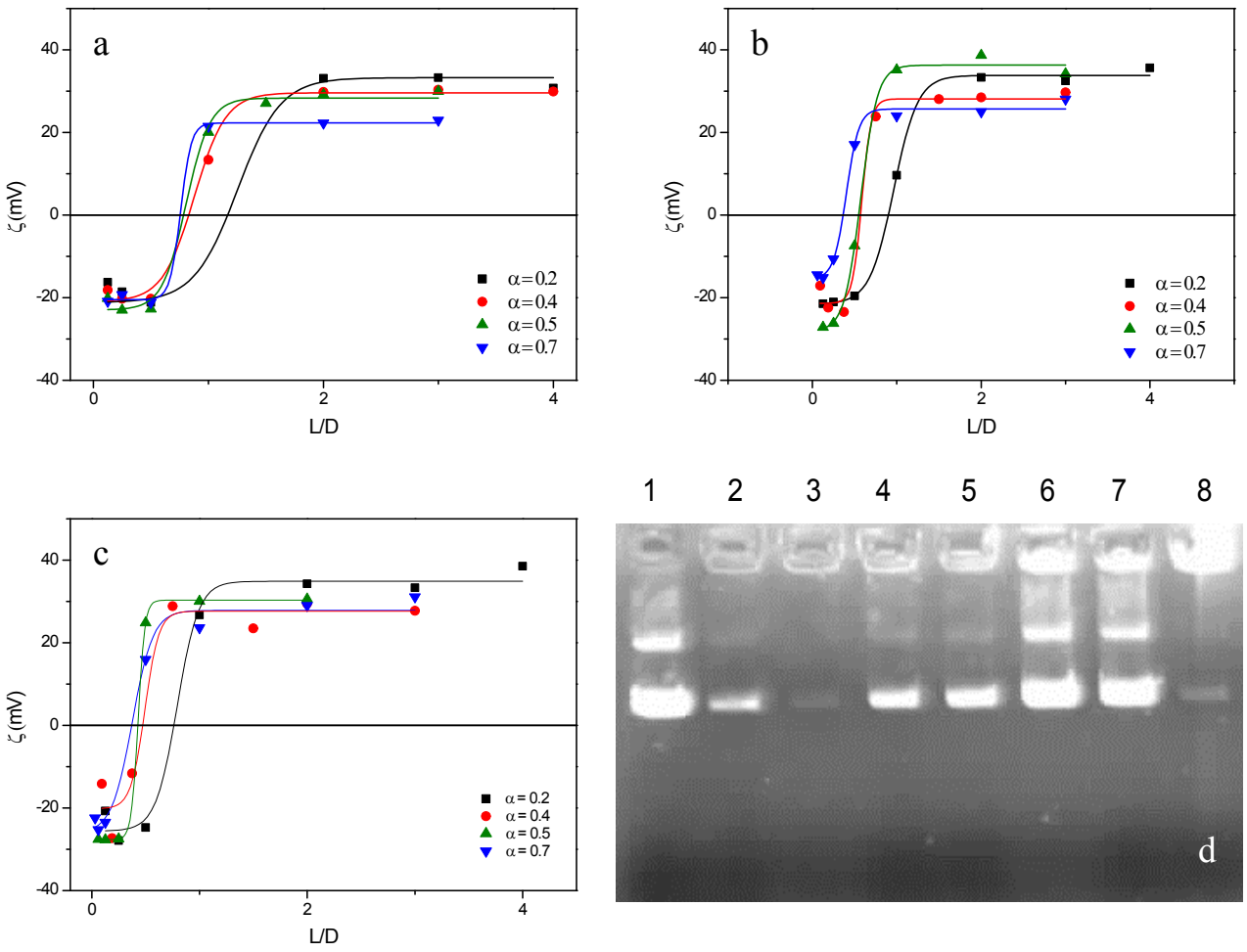

Fig. S1 (a-c) Plots of zeta potential (ζ) against the lipoplex nano-aggregate composition (L/D) at several GCL composition (α): (a) $(C_{16}Am)_2(C_2O)$/DOPE-pDNA; (b) $(C_{16}Am)_2(C_2O)_2$/DOPE-pDNA; (c) $(C_{16}Am)_2(C_2O)_3$/DOPE-pDNA. Errors are within ± 5%. (d) Gel electrophoresis retardation of pDNA (Lane 1 and 6) by complexing them with $(C_{16}Am)_2(C_2O)$/DOPE at $\alpha = 0.7$, for $\rho_{eff} = 1$ (Lane 2) and 1.5 (Lane 3); $(C_{16}Am)_2(C_2O)_2$/DOPE at $\alpha = 0.4$, for $\rho_{eff} = 1$ (Lane 4) and 1.5 (Lane 5) and $(C_{16}Am)_2(C_2O)_3$/DOPE at $\alpha = 0.7$, for $\rho_{eff} = 1.5$ (Lane 7) and 2 (Lane 8).

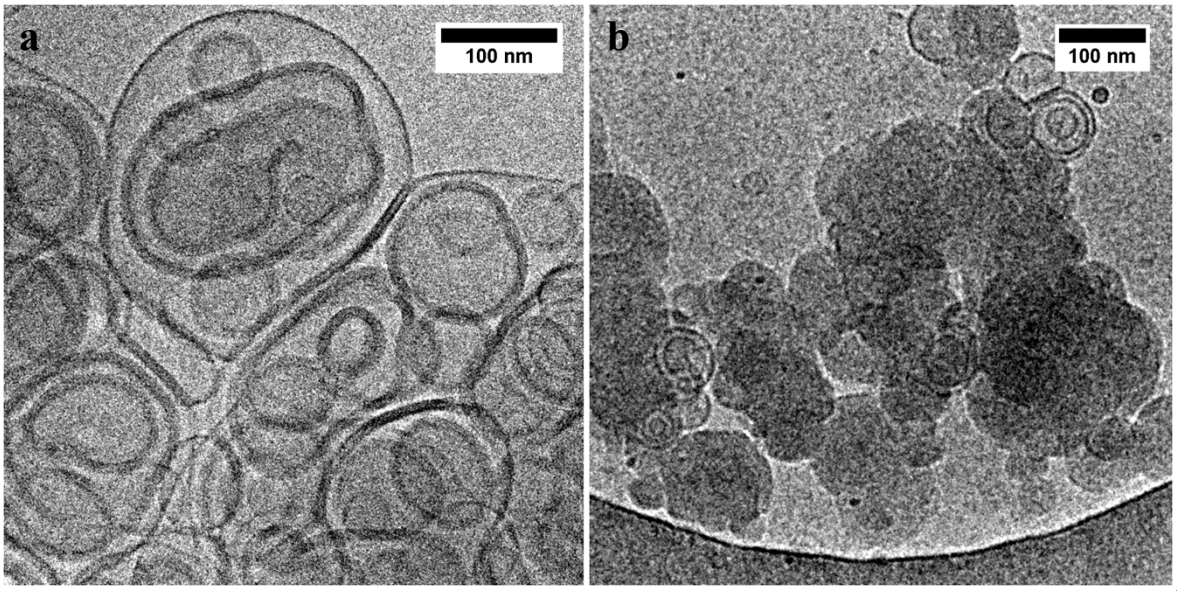

Fig. S2 A selection of Cryo-TEM micrographs showing a general view of the $(C_{16}Am)_2(C_2O)_2$/DOPE-pDNA lipoplex nano-aggregates at $\rho_{eff} = 1.5$ and at several GCL compositions (α). (a) $\alpha = 0.2$ and (b) $\alpha = 0.5$.

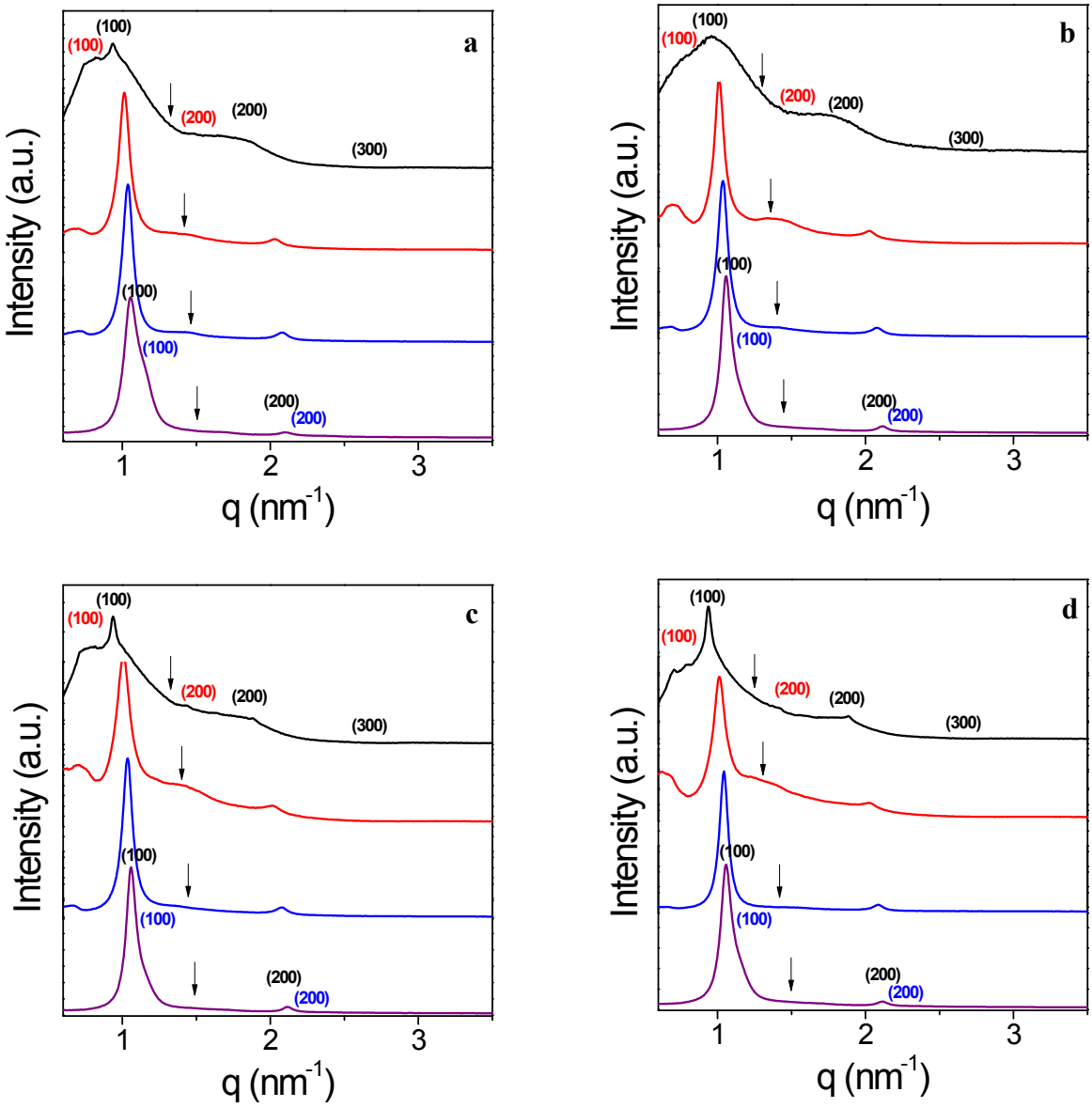

Fig. S3 SAXS diffractograms of $(C_{16}Am)_2(C_2O)$/DOPE-pDNA lipoplex nano-aggregates at several GCL compositions (α) and several effective charge ratios: (a) $\rho_{eff} = 2.0$; (b) $\rho_{eff} = 2.5$; (c) $\rho_{eff} = 3.0$; (d) $\rho_{eff} = 5.0$. In all the structures: black lines, $\alpha = 0.2$; red lines, $\alpha = 0.4$; blue lines, $\alpha = 0.5$; and purple lines, $\alpha = 0.7$. Miller indexes (hkl) correspond to the lamellar structures: red, $L_{\alpha,DOPE\ rich}$; black, $L_{\alpha\ main}$; and blue, $L_{\alpha\ GCL\ rich}$. Arrows indicate the pDNA-pDNA correlation peak.

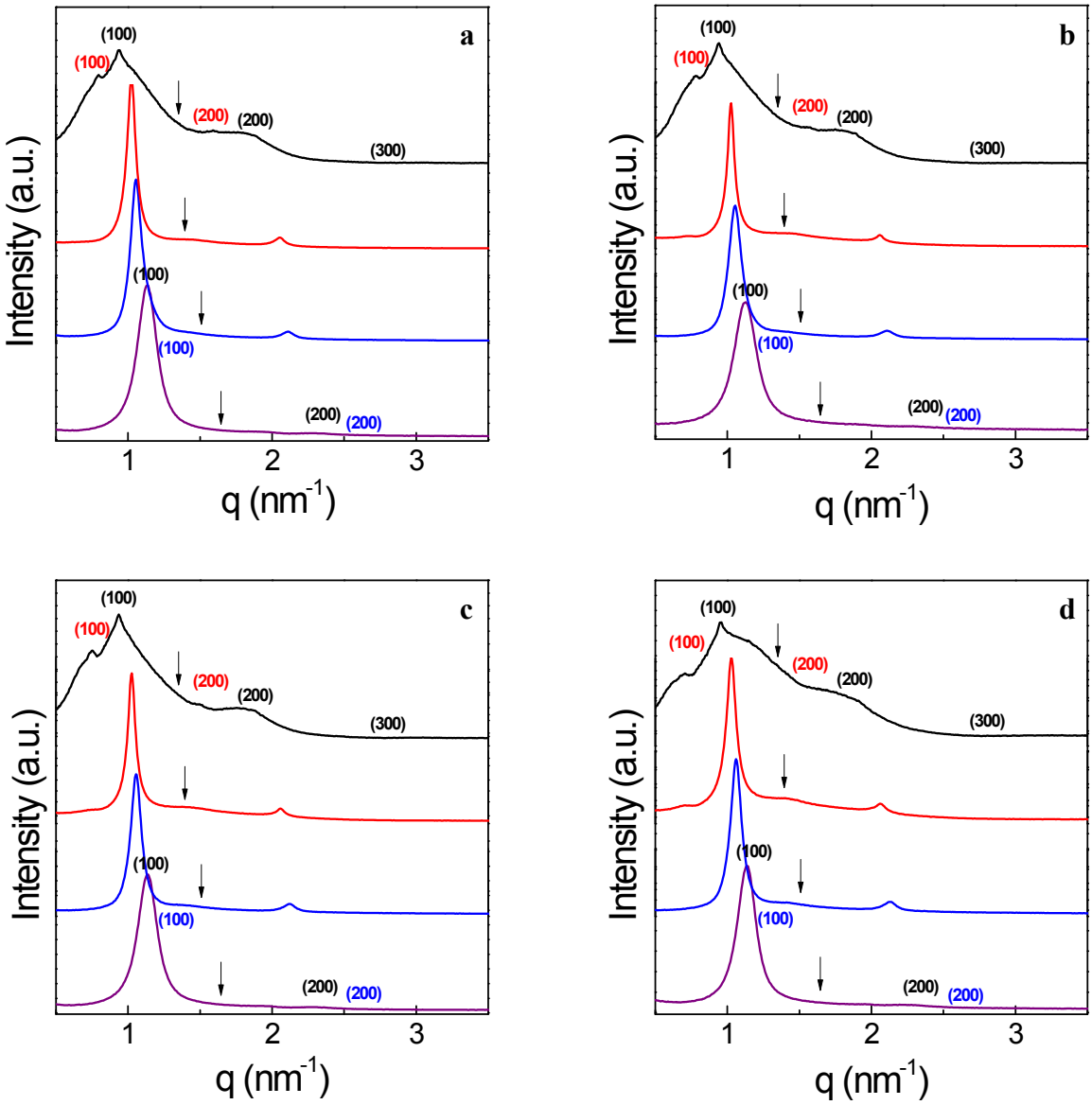

Fig. S4 SAXS diffractograms of $(C_{16}Am)_2(C_2O)_2$/DOPE-pDNA lipoplex nano-aggregates at several GCL compositions (α) and several effective charge ratios: (a) $\rho_{eff} = 2.0$; (b) $\rho_{eff} = 2.5$; (c) $\rho_{eff} = 3.0$; (d) $\rho_{eff} = 5.0$. In all the structures: black lines, $\alpha = 0.2$; red lines, $\alpha = 0.4$; blue lines, $\alpha = 0.5$; and purple lines, $\alpha = 0.7$. Miller indexes (hkl) correspond to the lamellar structures: red, $L_{\alpha,DOPE\ rich}$; black, $L_{\alpha\ main}$; and blue, $L_{\alpha\ GCL\ rich}$. Arrows indicate the pDNA-pDNA correlation peak.

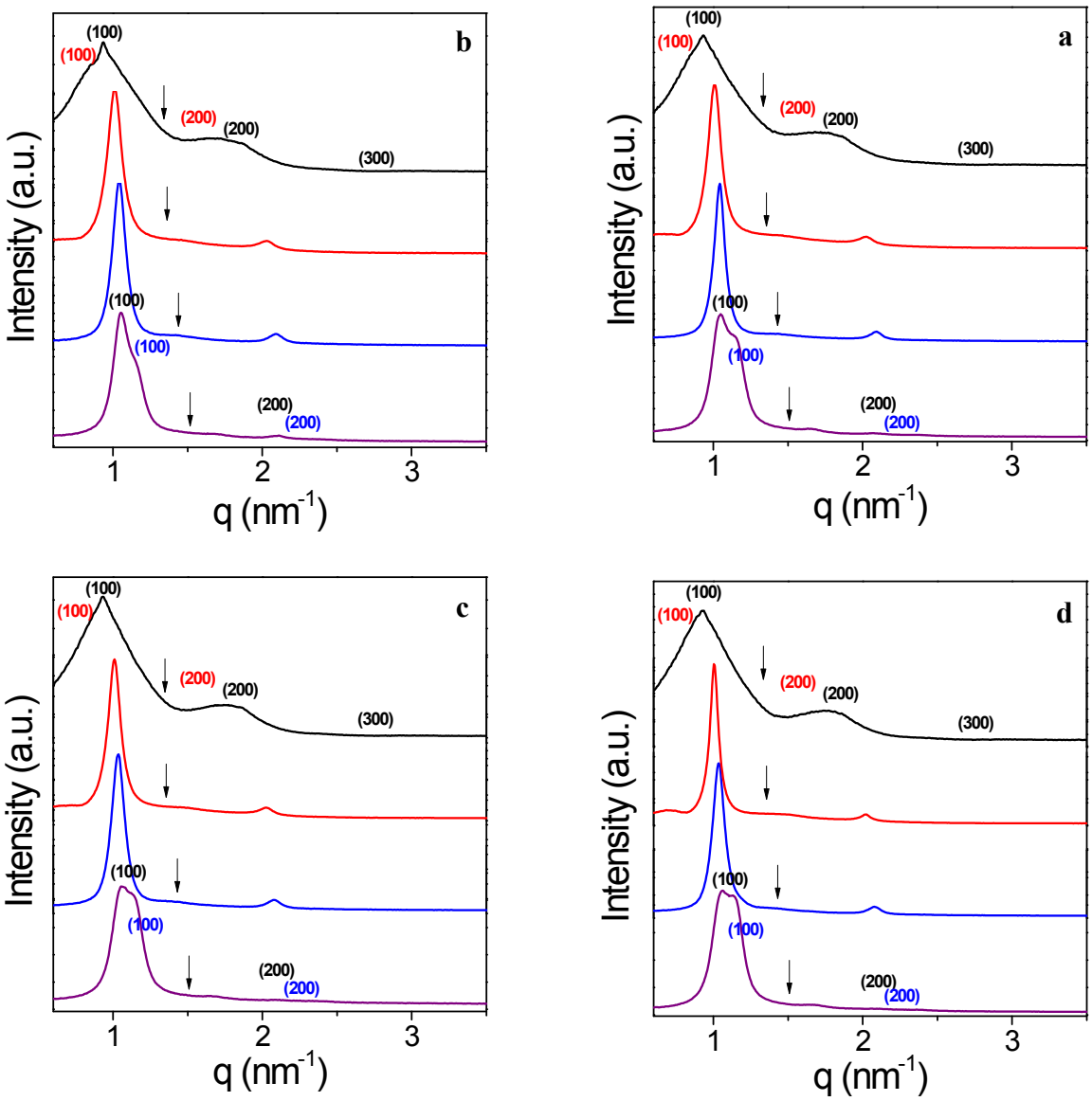

Fig. S5 SAXS diffractograms of $(C_{16}Am)_2(C_2O)_3$/DOPE-pDNA lipoplex nano-aggregates at several GL compositions (α) and several effective charge ratios: (a) $\rho_{eff} = 2.0$; (b) $\rho_{eff} = 2.5$; (c) $\rho_{eff} = 3.0$; (d) $\rho_{eff} = 5.0$. In all the structures: black lines, $\alpha = 0.2$; red lines, $\alpha = 0.4$; blue lines, $\alpha = 0.5$; and purple lines, $\alpha = 0.7$. Miller indexes (hkl) correspond to the lamellar structures: red, $L_{\alpha,DOPE\ rich}$; black, $L_{\alpha\ main}$; and blue, $L_{\alpha\ GCL\ rich}$. Arrows indicate the pDNA-pDNA correlation peak.

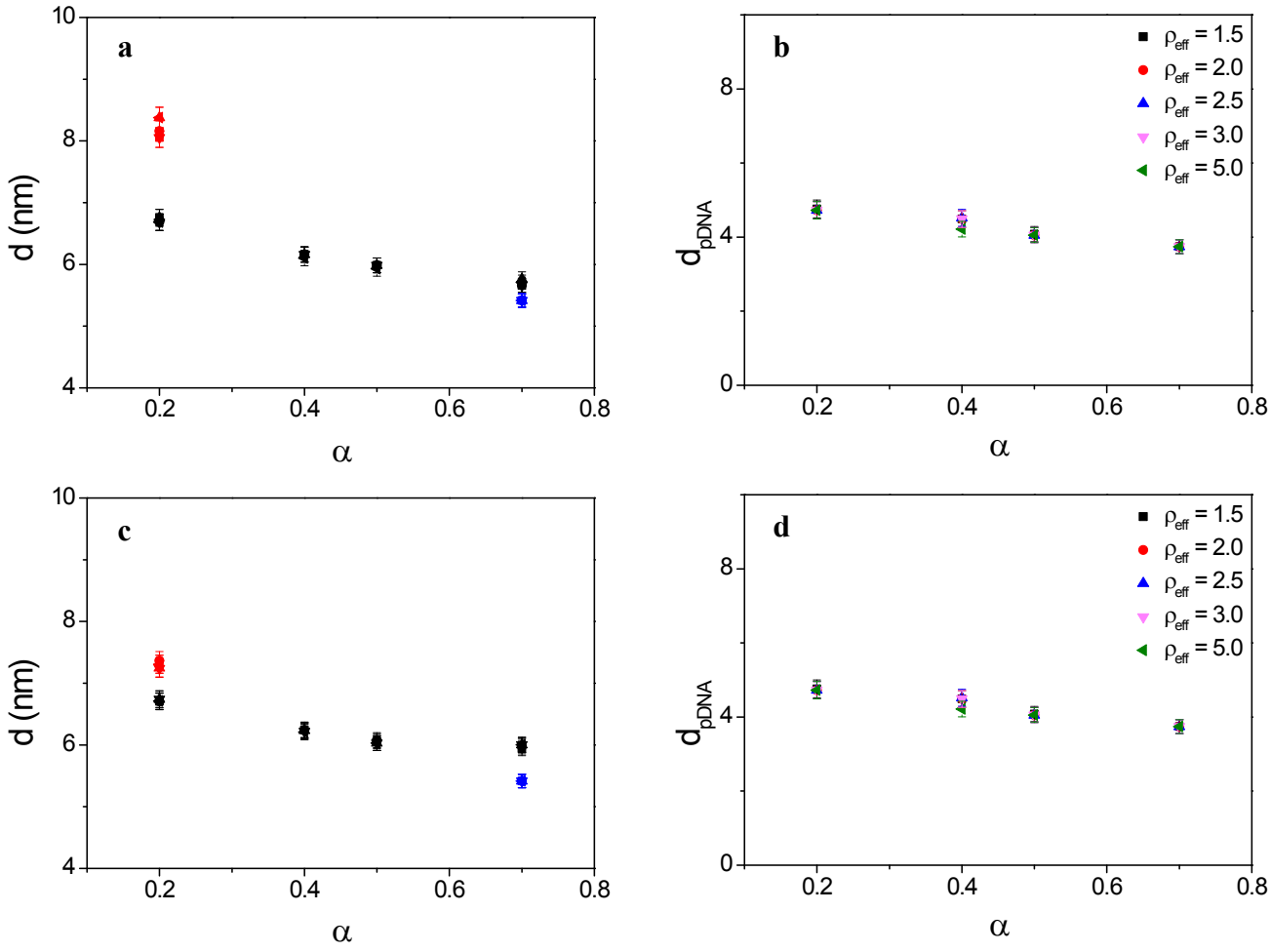

Fig. S6 (a, c) Plots of the periodic distance of the lamellar structure (d) for $(C_{16}Am)_2(C_2O)_n$/DOPE-pDNA lipoplex nano-aggregates as a function of GCL composition (α) at several effective charge ratios (ρ_{eff}): red symbols, $L_{\alpha,DOPE\ rich}$ structure; black symbols, $L_{\alpha\ main}$ structure; and blue symbols, $L_{\alpha\ GCL\ rich}$ structure. In all the structures: squares, ρ_{eff} = 1.5; circles, ρ_{eff} = 2.0; up triangles, ρ_{eff} = 2.5; down triangles, ρ_{eff} = 3.0; and left triangles, ρ_{eff} = 5.0. (b, d) Plots of the distance d_{pDNA} for $(C_{16}Am)_2(C_2O)_n$/DOPE-pDNA nano-aggregates as a function of GCL composition (α) at several effective charge ratios (ρ_{eff}). In the figure: (a, b) $(C_{16}Am)_2(C_2O)_2$/DOPE-pDNA; (c, d) $(C_{16}Am)_2(C_2O)_3$/DOPE-pDNA.

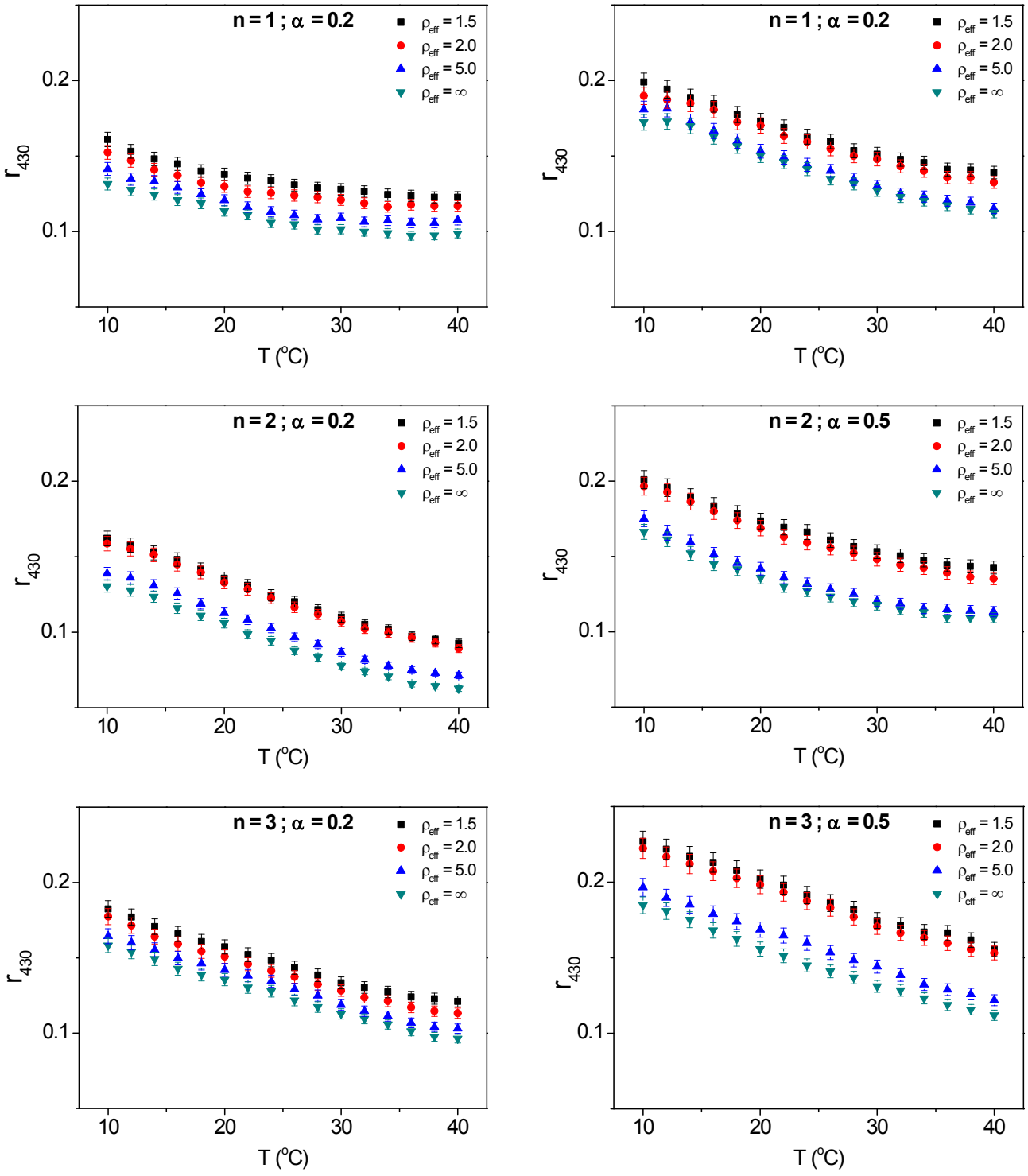

Fig. S7 Fluorescence anisotropy at 430 nm, r_{430}, of DPH as a function of temperature for $(C_{16}Am)_2(C_2O)_n$/DOPE-pDNA lipoplex-type nano-aggregates with n = 1, 2 or 3, at various effective charge ratios (ρ_{eff}). Values at $\rho_{eff} = \infty$ correspond to $(C_{16}Am)_2(C_2O)_n$/DOPE liposomes in the absence of pDNA. Errors by light scattering are less than 3%.

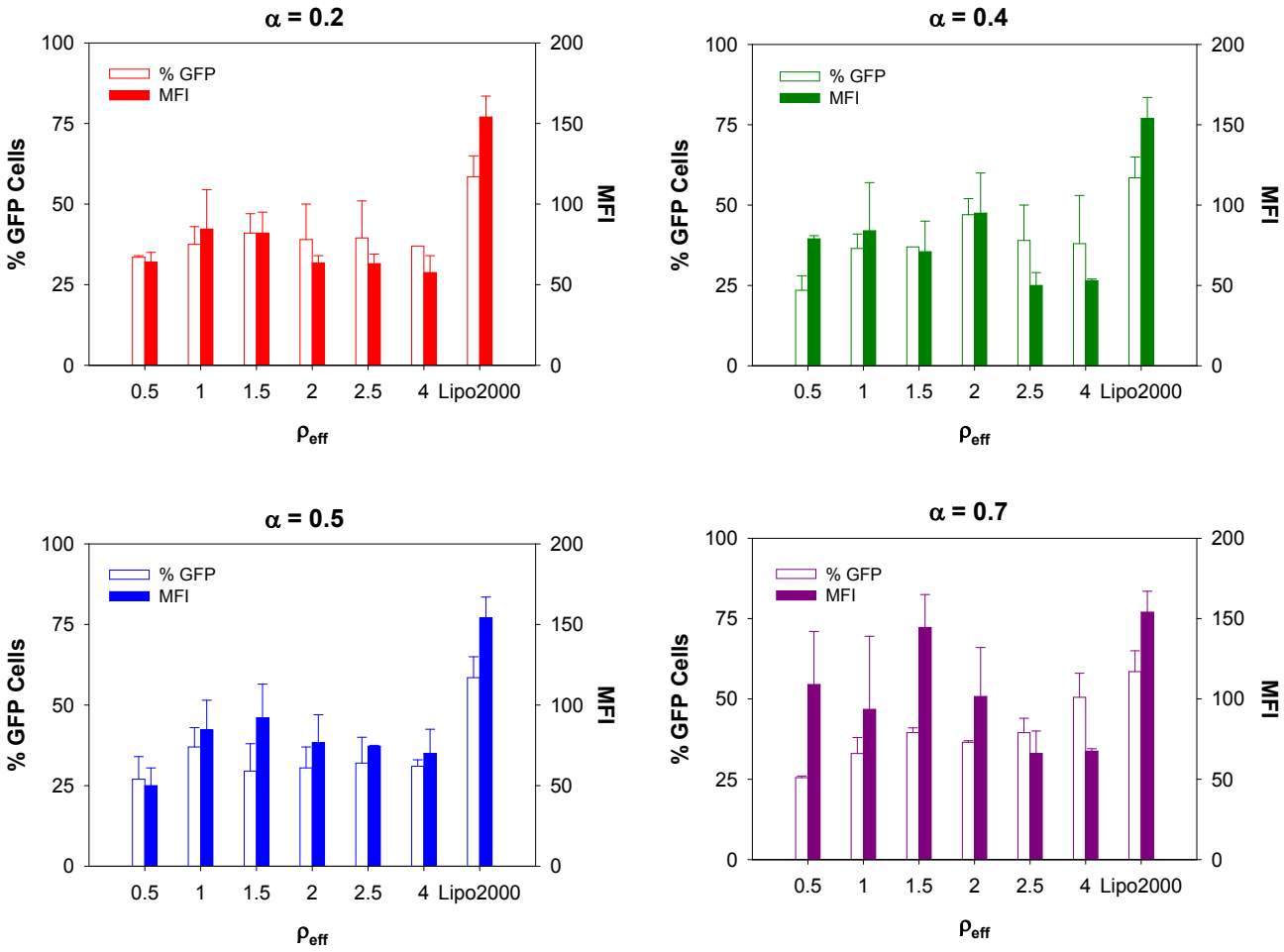

Fig. S8 Transfection of pEGFP-C3 in HEK293T cells in absence of serum (-FBS-FBS) using lipoplexes of $(C_{16}Am)_2(C_2O)$/DOPE at α = 0.2, 0.4, 0.5 and 0.7 and ρ_{eff} = 0.5, 1, 1.5, 2, 2.5 and 4. Experiments were performed using 0.8 µg pDNA per well. Lipo2000 was used as positive control.

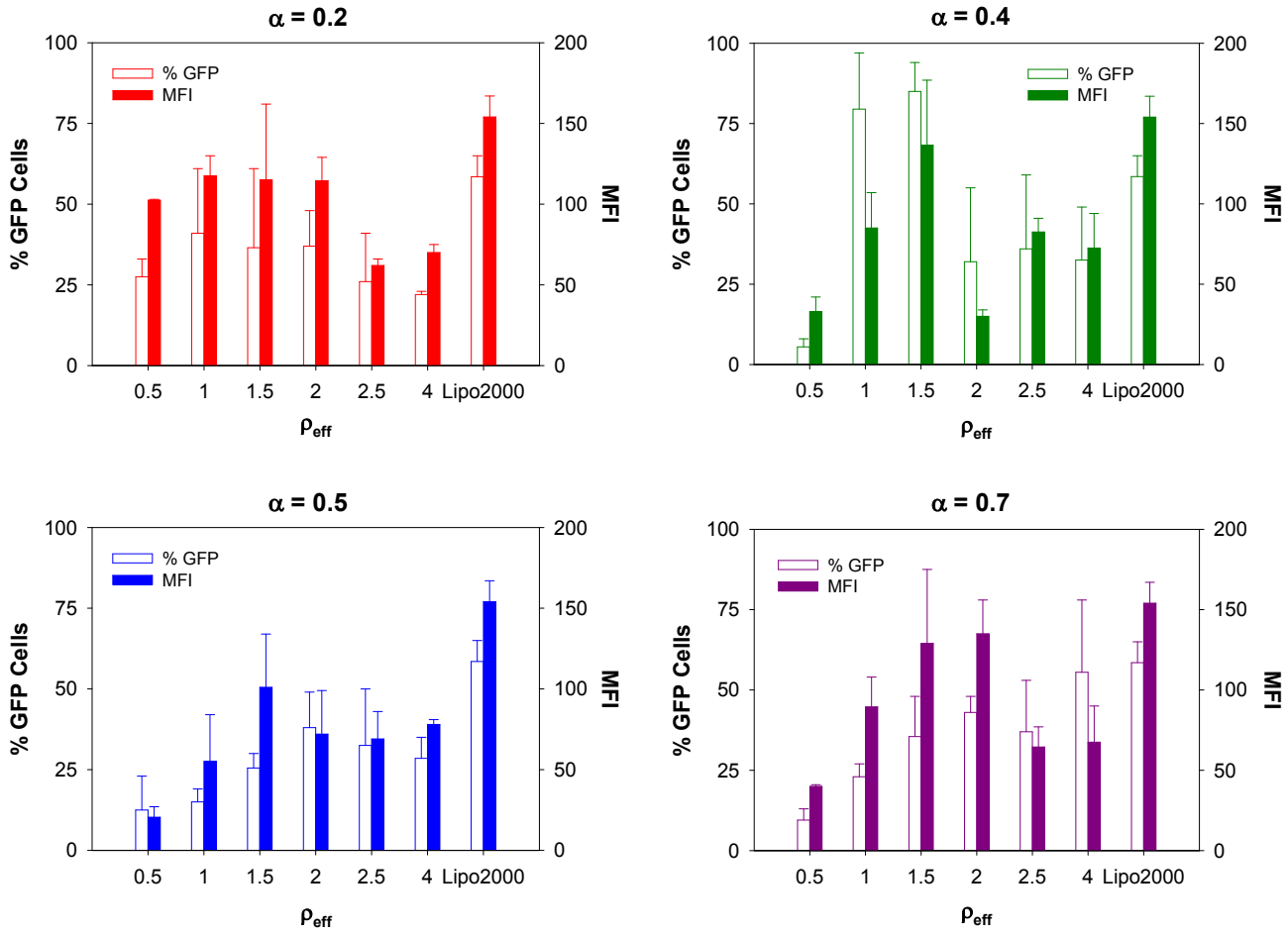

Fig. S9 Transfection of pEGFP-C3 in HEK293T cells in absence of serum (-FBS-FBS) using lipoplexes of $(C_{16}Am)_2(C_2O)_2$/DOPE at α = 0.2, 0.4, 0.5 and 0.7 and ρ_{eff} = 0.5, 1, 1.5, 2, 2.5 and 4. Experiments were performed using 0.8 µg pDNA per well. Lipo2000 was used as positive control.

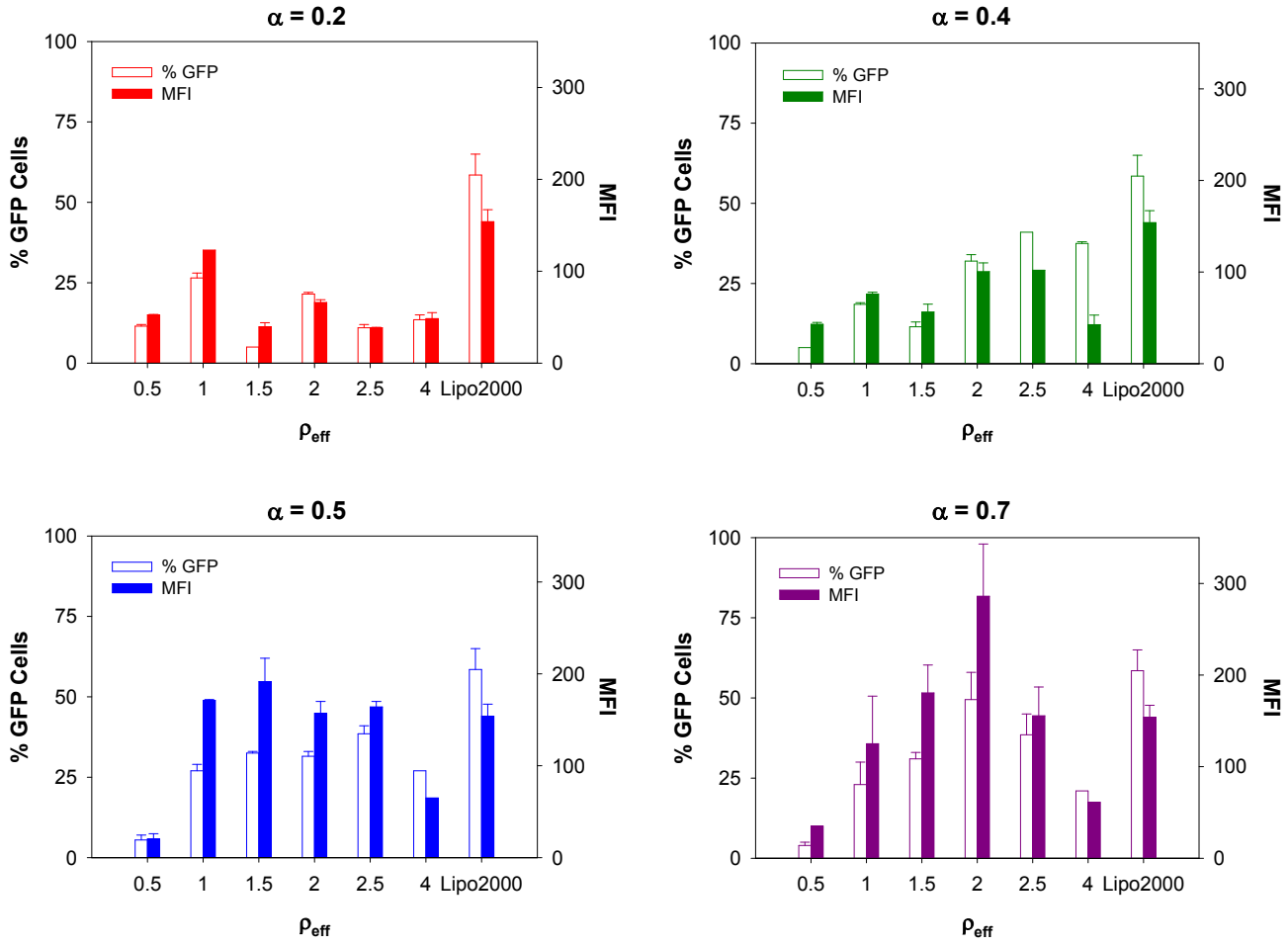

Fig. S10 Transfection of pEGFP-C3 in HEK293T cells in absence of serum (-FBS-FBS) using lipoplexes of $(C_{16}Am)_2(C_2O)_3$/DOPE at α = 0.2, 0.4, 0.5 and 0.7 and ρ_{eff} = 0.5, 1, 1.5, 2, 2.5 and 4. Experiments were performed using 0.8 µg pDNA per well. Lipo2000 was used as positive control.

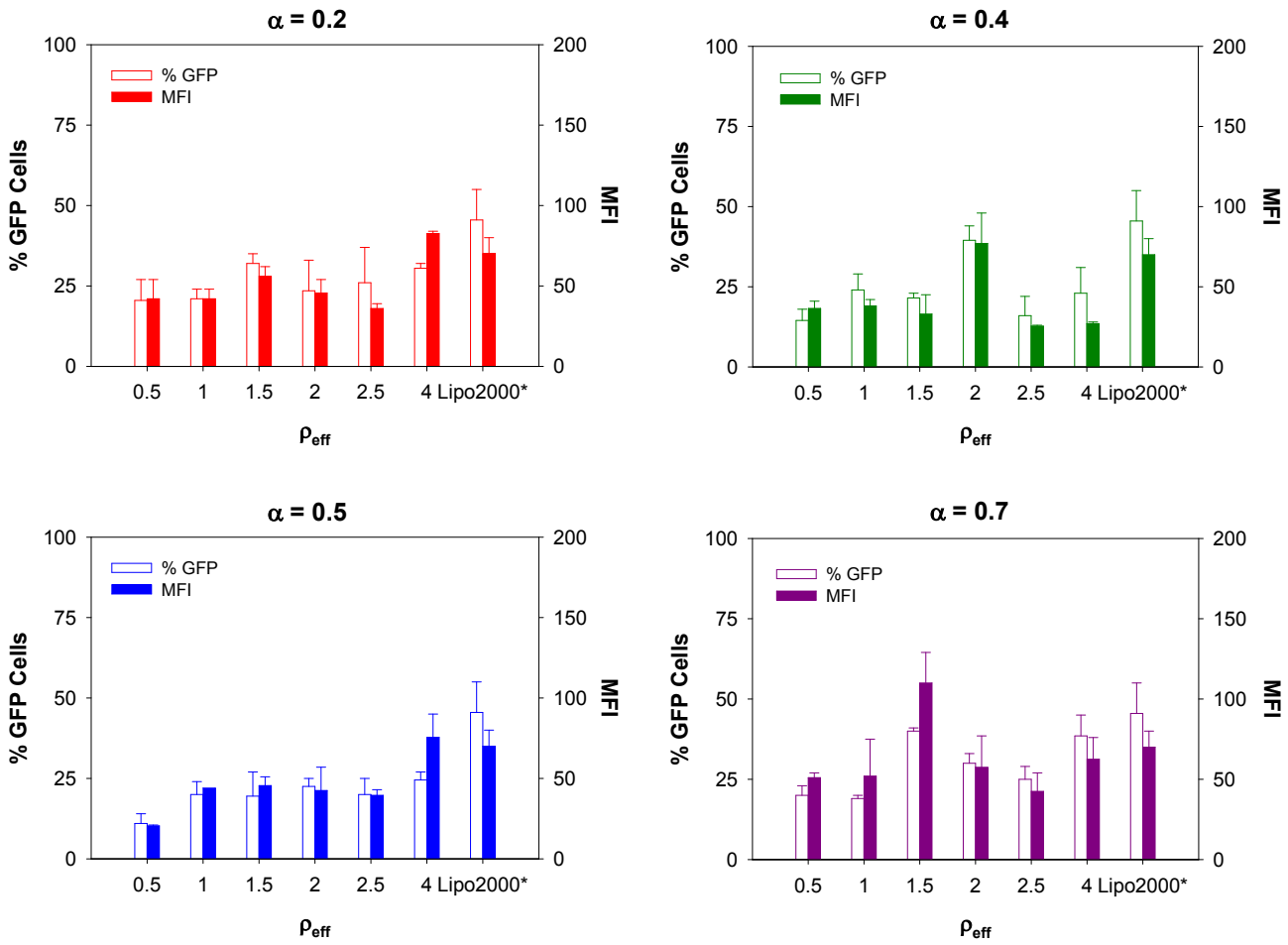

Fig. S11 Transfection of pEGFP-C3 in HEK293T cells in presence of serum (-FBS+FBS) using lipoplexes of $(C_{16}Am)_2(C_2O)$/DOPE at α = 0.2, 0.4, 0.5 and 0.7 and ρ_{eff} = 0.5, 1, 1.5, 2, 2.5 and 4. Experiments were performed using 0.8 µg pDNA per well. Lipo2000* was used as positive control.

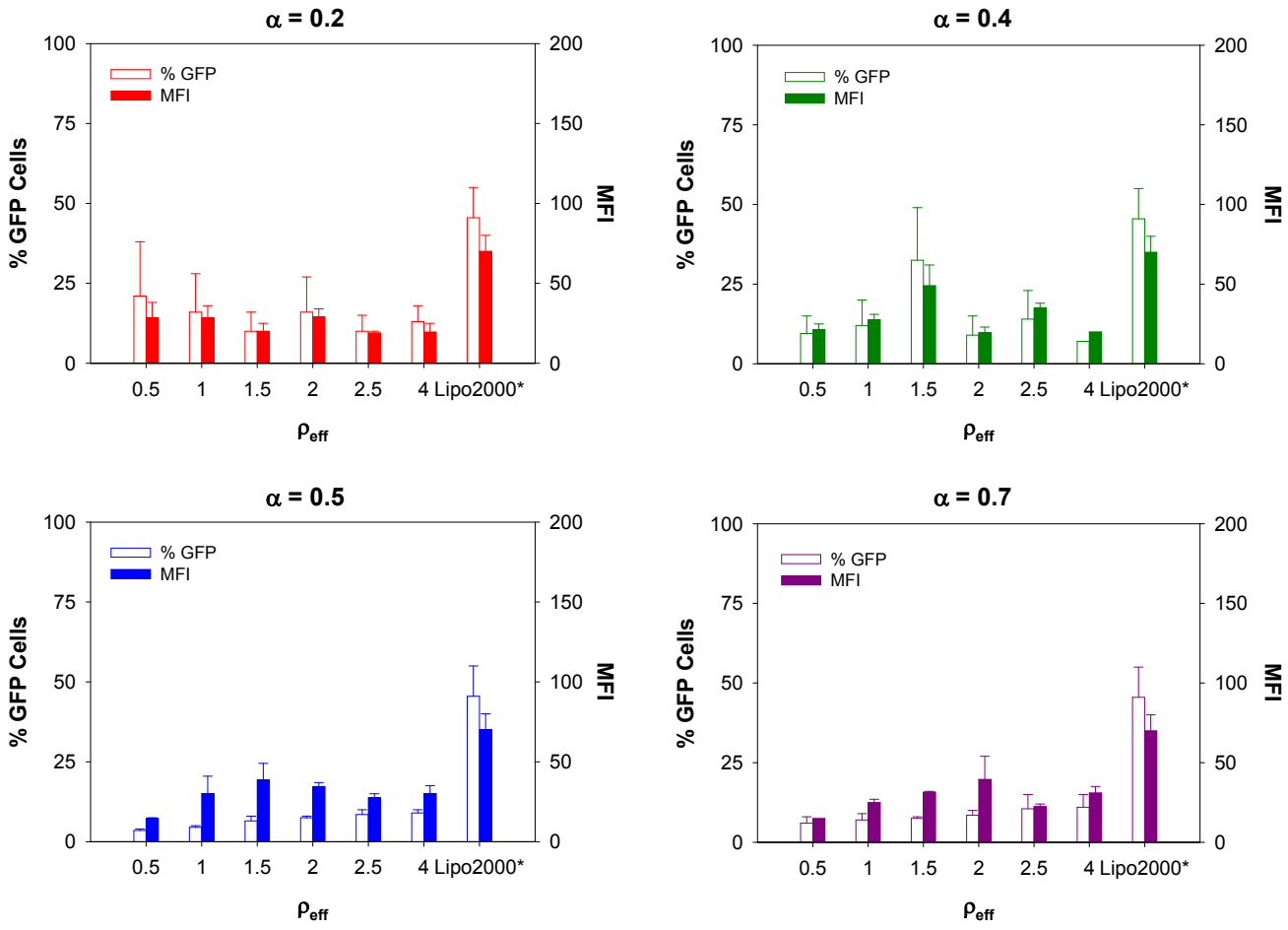

Fig. S12 Transfection of pEGFP-C3 in HEK293T cells in presence of serum (-FBS+FBS) using lipoplexes of $(C_{16}Am)_2(C_2O)_2$/DOPE at α = 0.2, 0.4, 0.5 and 0.7 and ρ_{eff} = 0.5, 1, 1.5, 2, 2.5 and 4. Experiments were performed using 0.8 µg pDNA per well. Lipo2000* was used as positive control.

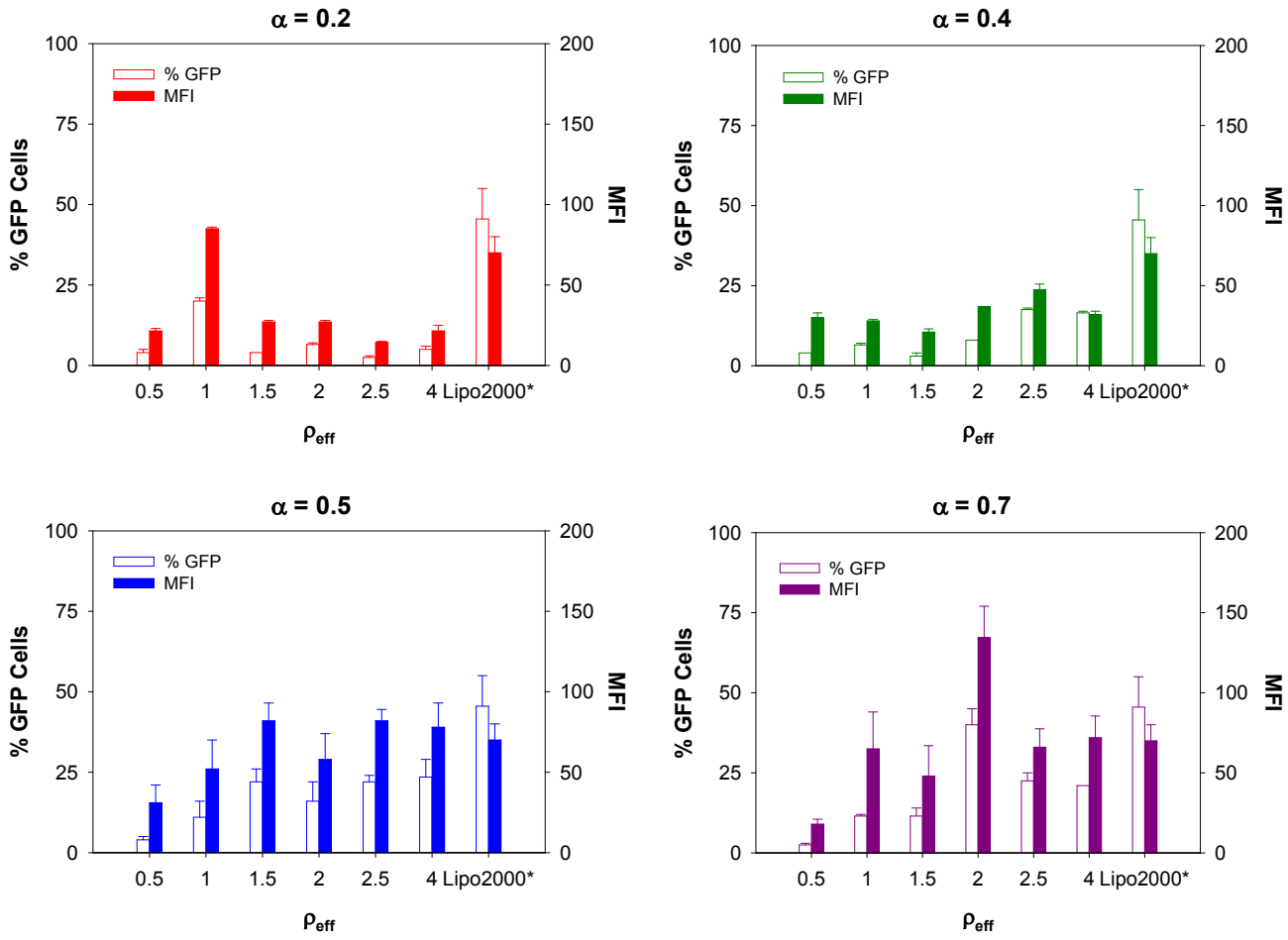

Fig. S13 Transfection of pEGFP-C3 in HEK293T cells in presence of serum (-FBS+FBS) using lipoplexes of $(C_{16}Am)_2(C_2O)_3$/DOPE at α = 0.2, 0.4, 0.5 and 0.7 and ρ_{eff} = 0.5, 1, 1.5, 2, 2.5 and 4. Experiments were performed using 0.8 µg pDNA per well. Lipo2000* was used as positive control.

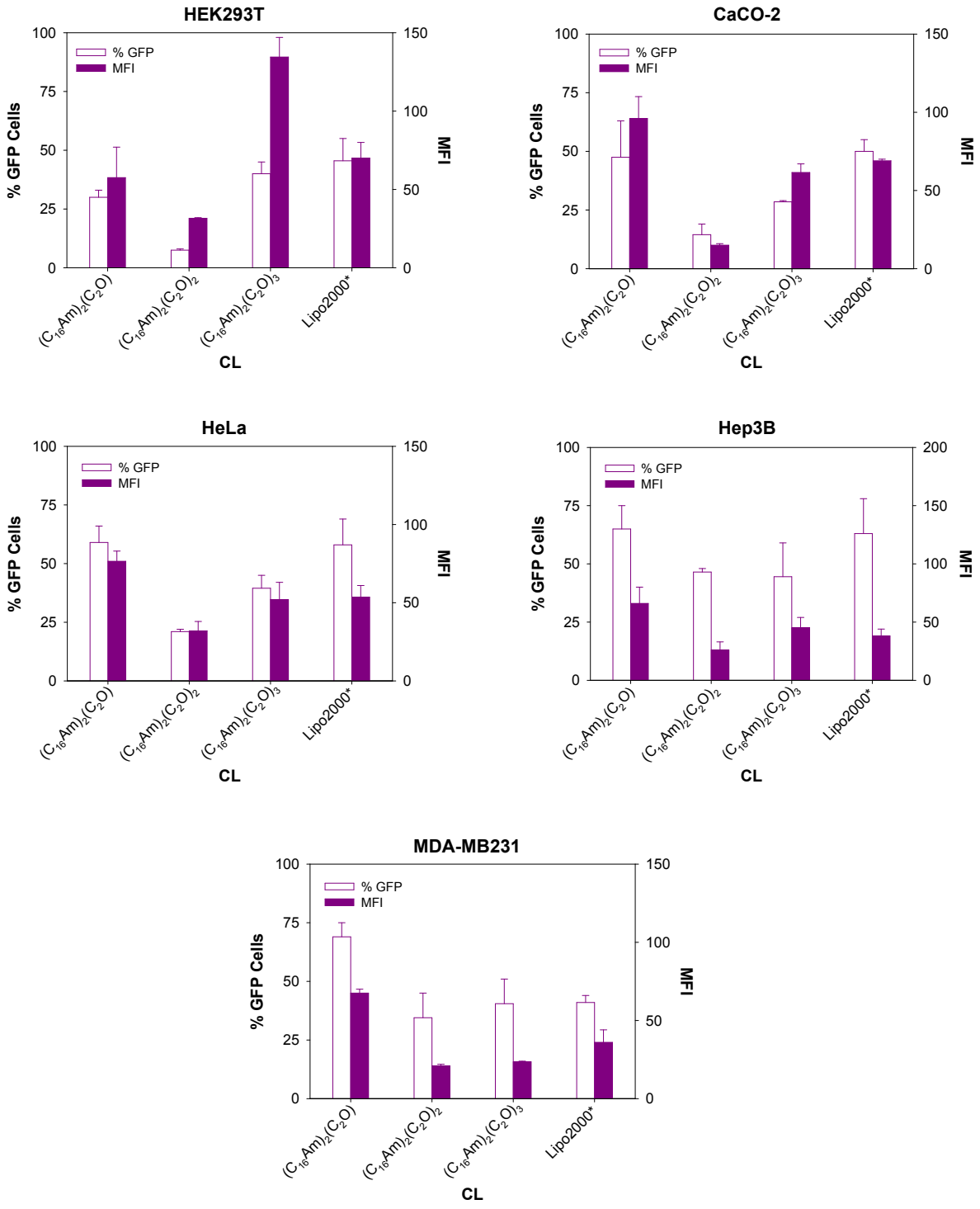

Fig. S14 Transfection of pEGFP-C3 in various cell lines in presence of serum (-FBS+FBS) using lipoplexes at α = 0.7 and ρ_{eff} = 2, 1.5 and 2 of $(C_{16}Am)_2(C_2O)$/DOPE, $(C_{16}Am)_2(C_2O)_2$/DOPE and $(C_{16}Am)_2(C_2O)_3$/DOPE, respectively. Experiments were performed using 0.8 µg pDNA per well. Lipo2000* was used as positive control.

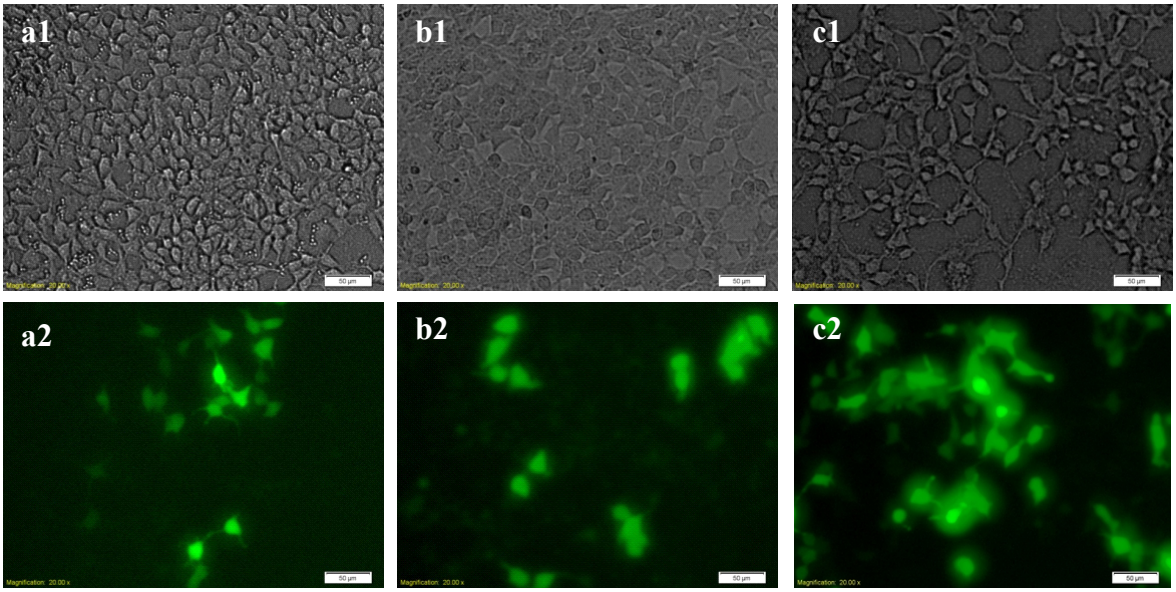

Fig. S15 Representative bright field (a1-c1) and fluorescence images (a2-c2) of HEK293T cells transfected with [$(C_{16}Am)_2(C_2O)$/DOPE-pDNA] prepared at optimized α = 0.7 and ρ_{eff} = 1.5 (a1, a2); [$(C_{16}Am)_2(C_2O)_2$/DOPE-pDNA] prepared at optimized α = 0.4 and ρ_{eff} = 1.0 (b1, b2) and [$(C_{16}Am)_2(C_2O)_3$/DOPE-pDNA] prepared at optimized α = 0.7 and ρ_{eff} = 2.0 (c1, c2) in absence of serum (-FBS-FBS). Experiments were performed using 0.8 μg pDNA per well. Scale bar is 50 μm.

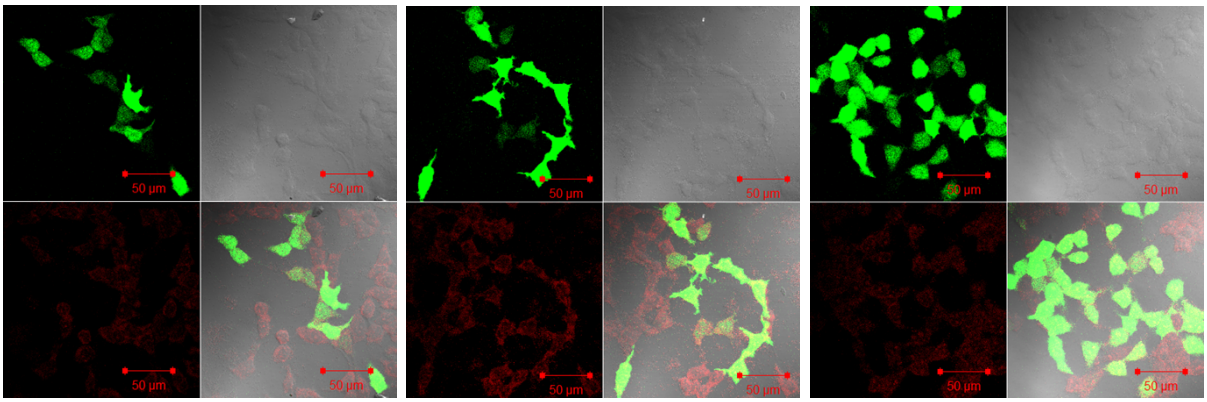

Fig. S16 Representative confocal images of HEK293T cells transfected with [$(C_{16}Am)_2(C_2O)$/DOPE-pDNA] prepared at optimized α = 0.7 and ρ_{eff} = 1.5 (a1-a4); [$(C_{16}Am)_2(C_2O)_2$/DOPE-pDNA] prepared at optimized α = 0.4 and ρ_{eff} = 1.0 (b1-b4) and [$(C_{16}Am)_2(C_2O)_3$/DOPE-pDNA] prepared at optimized α = 0.7 and ρ_{eff} = 2.0 (c1-c4) in absence of serum (-FBS-FBS). Panel (a1-c1), (a2-c2), (a3-c3) and (a4-c4) represent GFP expression in cells, bright field, PI staining and overlapped images, respectively. Scale bar is 50 µm.

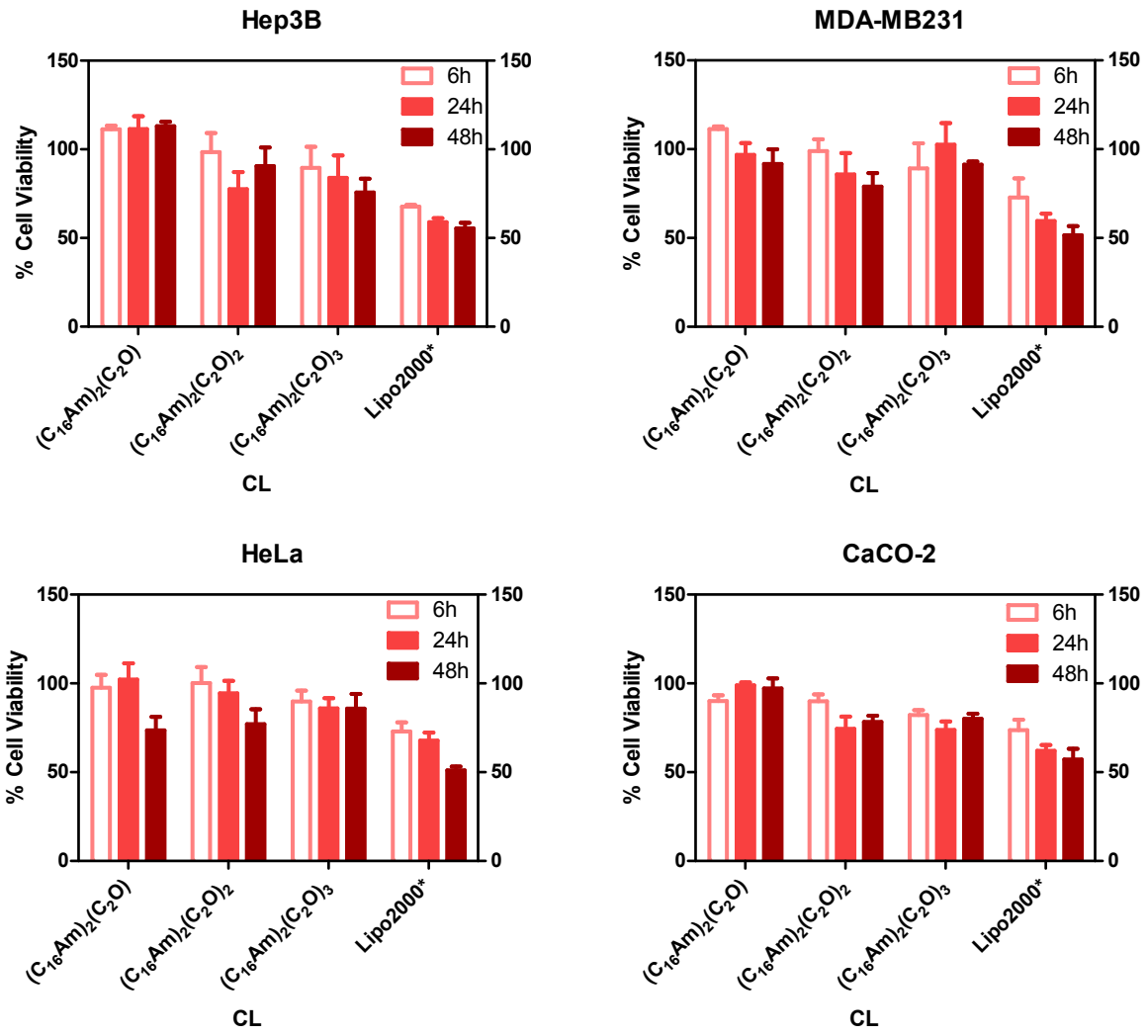

Fig. S17 Cell viability assay of CaCO-2, HeLa, Hep3B and MDA-MB231 cells transfected in presence of serum (-FBS+FBS) with lipoplexes prepared at the optimized formulations: [$(C_{16}Am)_2(C_2O)$/DOPE-pDNA] at α = 0.7 and ρ_{eff} = 1.5; [$(C_{16}Am)_2(C_2O)_2$/DOPE-pDNA] at α = 0.4 and ρ_{eff} = 1 and; [$(C_{16}Am)_2(C_2O)_3$/DOPE-pDNA] at α = 0.7 and ρ_{eff} = 2. Experiments were performed by incubating lipoplexes at different time points of 6, 24 and 48 h.